Distribution Agreement

In presenting this thesis as a partial fulfillment of the requirements for a degree from Emory University, I hereby grant to Emory University and its agents the non-exclusive license to archive, make accessible, and display my thesis in whole or in part in all forms of media, now or hereafter know, including display on the World Wide Web. I understand that I may select some access restrictions as part of the online submission of this thesis. I retain all ownership rights to the copyright of the thesis. I also retain the right to use in future works (such as articles or books) all or part of this thesis.

Satvik Hadigal April 13, 2011

Affect of form deprivation on visual thresholds in *nob* mice

by

Satvik Hadigal

Dr. Machelle Pardue
Adviser

Department of Biology

Dr. Machelle Pardue

Adviser

Dr. Michael Iuvone

Committee Member

Dr. Robert Liu

Committee Member

Dr. Iain Shepherd

Committee Member

April 13, 2011

Affect of form deprivation on visual thresholds in *nob* mice

By

Satvik Hadigal

Dr. Machelle Pardue

Adviser

An abstract of
a thesis submitted to the Faculty of Emory College of Arts and Sciences
of Emory University in partial fulfillment
of the requirements of the degree of
Bachelor of Sciences with Honors

Department of Biology

2011

Abstract

Affect of form deprivation on visual thresholds in *nob* mice

By Satvik Hadigal

Purpose: Form deprivation induces exaggerated eye growth that leads to myopia. This shift in refractive error may negatively impact visual function. In this study, visual function of WT mice was measured before and after form deprivation. These results were compared to *nob* mice which have a defect in the retinal ON-pathway to determine the role of ON pathway transmission in visual acuity and contrast sensitivity after form deprivation myopia.

Methods: Refractive development of eyes during form deprivation was measured using an IR photorefractor. Visual acuity and contrast sensitivity were measured using an optokinetic tracking device. Mouse eyes were form deprived using diffuser goggles mounted in frames attached to head pedestals. Baseline refractions and visual thresholds of mice were taken prior to goggling. *Nob* mice were followed for 2 weeks and WT mice were followed for 4 weeks. Refractions and visual threshold measurements were repeated at the final timepoint, after myopia development.

Reuslts: *Nob* mice had a higher myopic shift when compared to WT mice at 2 and 4 weeks of form deprivation, respectively. Baseline visual acuity and contrast sensitivity of *nob* mice were lower than WT mice. Visual acuity and contrast sensitivity of WT mice did not significantly change after myopia development; however visual acuity and contrast sensitivity of *nob* mice decreased significantly. While the control eyes of WT mice had stable visual thresholds between the two time points, the control eyes of *nob* mice increased in visual threshold.

Conclusion: *Nob* mice with defective ON pathways have increased susceptibility to form deprivation and an associated decrease in visual acuity and contrast sensitivity. A functional ON pathway is necessary in post-natal retinal development to achieve peak visual performance.

Affect of form deprivation on visual thresholds in *nob* mice

By

Satvik Hadigal

Dr. Machelle Pardue

Adviser

A thesis submitted to the Faculty of Emory College of Arts and Sciences
of Emory University in partial fulfillment
of the requirements of the degree of
Bachelor of Sciences with Honors

Department of Biology

2011

Acknowledgements

I first want to thank Dr. Machelle Pardue for diligently guiding me through the entire project, and for contributing her precious time to revisions made on this paper.

Hannah Park and Christopher Tan for helping me with data collection.

Table of Contents

Introduction:

Myopia is a refractive defect in the eye in which objects viewed in the distance appear blurred. Myopia is increasing in prevalence in many parts of the world. In many Asian groups the incidence of myopia may be between 80 to 90% (Miller 2003). Myopia is emerging as a global health problem because of the costs of correcting refractive error (Economics 2004). Although myopia treatments exist, high-levels of myopia are susceptible to several complications such as choroidal degenerative changes (Miller 2003), high incidence of retinal detachment (Miller 2003), glaucoma (Wu, Nemesure et al. 1999), retinal degeneration (Saw, Gazzard et al. 2005) and choroidal neovascularization (Cohen, Laroche et al. 1996).

Myopia is caused by mismatch between refractive power and axial length of the eye. The axial length is longer than the focal point of the eye, where the image is formed. In a normal eye the image is formed on the retina but in case of myopia, the image is formed in front of the retina.

Myopia is known to be caused by environmental and genetic contributions. Some of the environmental contributions in myopia formation are associated with color vision deficiencies (Qian, Chu et al. 2009), deficiency in fine detail (Khor, Fan et al. 2010), contrast sensitivity and brightness (Schaeffel 2006). Some of the genes that cause myopia are transforming growth factor beta 1 (TGFβ1) (Feldkaemper, Diether et al. 1999), pax6 (Liang, Hsi et al. 2011), 15q14, 15q25 (Hayashi, Yamashiro et al. 2011) and several more. Dopamine has also been shown to be related to myopia (Stone, Lin et al. 1989). Neither the brain (Troilo, Gottlieb et al. 1987) nor cues derived from accommodation (Schaeffel, Troilo et al. 1990) are necessary for the formation of myopia. Therefore, the underlying mechanism seems to be located in the retina (Schaeffel and Diether 1999).

When the retina detects a flawed image it releases growth signals via the retinal pigment epithelium to the sclera (Pardue, Faulkner et al. 2008). In an attempt to correct vision, the sclera grows and thins, increasing the axial length of the eye. Scleral thinning and tissue loss occur rapidly during development of myopia (Rada, Shelton et al. 2006). Scleral thinning is associated with net loss of matrix, smaller diameter collagen fibrils in the sclera, and reduced collagen production (Rada, Shelton et al. 2006) (Gentle, Liu et al. 2003).

The growth of the eye is guided by visual feedback with the ultimate aim being optimal focus of the retinal image. Previous studies have shown that brightness (Feldkaemper, Diether et al. 1999), high spatial frequency content of image (Hess, Schmid et al. 2006), and low contrast (Hess, Schmid et al. 2006) can cause myopia. However, it is unclear as to which particular image properties are responsible for the formation of myopia.

To understand the mechanism of myopia formation several animal models have been used such as chicks, tree shrews, guinea pigs, fish, and non-human primates with considerable success. However, each of these animal models has advantages and disadvantages. Avian eyes respond very well to environmental disruptions, developing considerable myopia within hours or days (Wallman and Winawer 2004). However, eyes of avian models do not sufficiently compare to that of a human's in terms of accommodation and anatomy. Primates are a mammalian model, but availability of primates is limited and myopia formation can take several weeks. Guinea pigs and tree shrews are also mammalian models that develop experimental myopia, but cannot easily provide genetic information. Mice, on the other hand, are promising myopia models where genetic and environmental studies can yield reliable information about mammals (Faulkner, Kim et al. 2007).

Form deprivation is a popular way to induce myopia in the laboratory setting. Form deprivation can be induced via frosted goggles or lid suture. Mouse eyes have been subjected to different forms of myopia induction mechanisms such as suturing the eye-lids and gluing a diffuser goggle to the fur around the eye. Both these mechanism have disadvantages. Lid-suturing increases intra-ocular pressure and may also change the corneal curvature of the eye thereby changing refractive measurements of eyes (Marsh-Tootle and Norton 1989). Gluing diffuser goggles to the eye requires the use of an Elizabethan collar which decreases the ability of grooming and subsequent formation of corneal ulcers (Faulkner, Kim et al. 2007). Hence, for this experiment, a method which ensures stability, comfort to the mice and ability to replace goggles whenever needed was used (Faulkner, Kim et al. 2007). This method uses an acrylic cube mounted via head pedestal that is attached to the skull of the mouse via surgery. The goggle is inserted into the cube and tightened with the help of a screw (Figure 1). The goggle can be removed whenever necessary during the experiment (Faulkner, Kim et al. 2007).

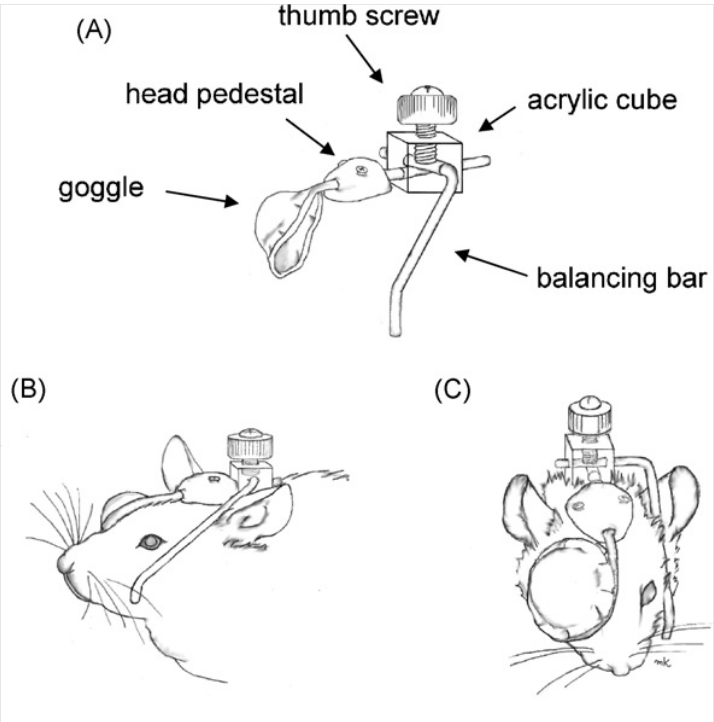

Figure 1. Form deprivation goggling in mice. (A) The whole apparatus shown indicating goggle, pedestal, screw and balancing bar. (B) Position of balancing bar on the left side. (C) Head of a mouse with the whole apparatus. Reprinted from Journal of Neuroscience Methods, 161, Faulkner, A., M. Kim, et al., Head-mounted goggles for murine form deprivation myopia, 97, Copyright (2007), with permission from Elsevier.

Retina

In mammals the retina is comprised of several layers of neurons (Figure 2). The innermost layer consists of ganglion cells and is bound by vitreous humor on one side and inner-plexiform layer on the other. The inner plexiform layer is composed of axons and synapses of bipolar cells, amacrine cells and horizontal cells. The inner plexiform layer is located interior to the cell bodies of amacrine, horizontal and bipolar cells which are located in the inner nuclear year. Photoreceptors synapse to bipolar cells in the outer plexiform layer. This layer is then surrounded by a final layer of photoreceptor cell bodies called the outer nuclear layer and includes rods and cones. These cells have protrusions called inner and outer segments where

phototransduction of light takes place. The retina is bound to retinal pigment epithelium (RPE) which lies inner to the choroid layer that serves the photoreceptors with blood vessels. The choroid is then bound by sclera, a white colored tissue which envelopes the entire structure of an eye.

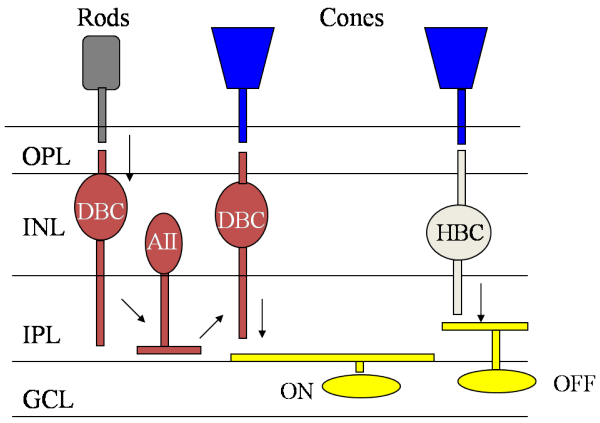

Figure 2. A schematic of a retina with rod and cone pathways. OPL; outer plexiform layer; INL: inner nuclear layer; IPL: inner plexiform layer; GCL: ganglion cell layer; DBC: depolarizing ON bipolar cell; AII: AII amacrine cell; HBC: hyperpolarizing OFF bipolar cell.

Light photons from the visual image reach the outer segments of the photoreceptor layer and excite specific molecules called opsins. These photoactivated opsins undergo phototransduction cascade which hyperpolarizes photoreceptors and transmits the signal to the inner nuclear layer. Cone photoreceptors have two to three specific opsins which can detect different wavelengths which allow for perception of color. Rod photoreceptors have a single photopigment, rhodopsin. Rods are sensitive to single photons and thus functionin darker environments, whereas cones have much less sensitivity and function in brighter environments. Cone photoreceptors are connected to ON and OFF bipolar cells and rod photoreceptors are connected to a separate set of ON bipolar cells (Figure 2). Amacrine cells connect bipolar cells of rods and cones. Signals from ON-bipolar (DBC-depolarizing bipolar cell) pathway are transferred to ON ganglion pathway. Signals from OFF-bipolar (HBC-hyperpolarizing bipolar

cell) pathway are transferred to OFF ganglion pathway (Figure 2). The ganglion cell layer, the innermost layer of the retina is connected to the optic nerve and passes the visual information to the brain.

Although mice provide a better comparison to humans than some other myopia models, there are some key differences between the two species. Mice have an abundance of rods (97%) than cones. Since mice are nocturnal animals additional rods aid in darker environments. While humans have a similar number of rods (~95%), the cones are allocated in a specialized region in the retina called the macula. Macula is used to detect fine detail. Mice do not have a macula.

Nob mice and ON pathway

A visual stimulus is initiated by photons which activate specific opsins and the phototransduction pathway in the photoreceptors. The signal is transferred to the bipolar cells in the inner nuclear layer. The rods have a single bipolar pathway called the ON bipolar pathway. Cones have two bipolar pathways called the ON bipolar pathway and OFF bipolar pathway. The rod bipolar pathway is used in scotopic vision and the cone bipolar pathways are used in photopic vision. Mutant mouse models provide an opportunity to functionally test specific elements of proposed visual pathways. In this experiment *nob* mice, which have a loss of function of ON pathway are used. Disruption of ON and OFF pathways may affect eye growth and it has been shown that ON pathway defect influences refractive development (Pardue, Faulkner et al. 2008). *Nob* mice carry a null mutation in the *Nyx* gene, which encodes the protein nyctalopin located on the post-synaptic side of the photoreceptor-to-ON bipolar cell synapse (Morgans, Ren et al. 2006). Electroretinogram (ERG) and behavioral tests have shown that *nob* mice have a loss of visual transmission in the ON-pathway of rods and cones, however

photoreceptor function remains normal (Pardue, McCall et al. 1998). Hence the dendrites of the bipolar cells do not pick up the signal given off by the photoreceptors. In functional pathways ON-bipolar cells pick up the signal via mGluR6 receptor which then follows a signal transduction cascade via G-protein coupling. Since ON-bipolar cells are not activated, nyctalopin is proposed to play a crucial role in this cascade mechanism (Gregg, Mukhopadhyay et al. 2003).

Presynaptically, the photoreceptors communicate the presence of light by reducing the tonic release of glutamate. Postsynaptically, this change is detected by two classes of bipolar cells, sign-conserving and sign inverting. The sign inverting depolarizes while the sign-conserving hyperpolarizes bipolar cells. Since, the ON-pathway defect compromises depolarizing bipolar cells, only the hyperpolarizing bipolar cells of cones is proposed to have complete function (Gregg, Mukhopadhyay et al. 2003). Hence, visual capability in scotopic (dark) conditions is greatly reduced. Interestingly, *nob* mice are found to be similar to complete form of human X-linked congenital night blindness (CSNB1). *Nob* mice have decreased sensitivity to light just like patients with CSNB1 (Gregg, Mukhopadhyay et al. 2003).

The ON pathway defect in *nob* mice is also proposed to lead to lower levels of dopamine in the retina (Pardue, Faulkner et al. 2008). Dopamine is a catecholamine neurotransmitter in the retina. Dopamine release is stimulated by light exposure using the ON pathway (Boatright, Gordon et al. 1994). Dopamine is metabolized into DOPAC in neurons. Interestingly, decreased levels of dopamine and DOPAC are linked to form deprivation myopia (Stone, Lin et al. 1989).

Refractions of eye

The progression of myopia can be measured using a photorefractor which measures the refractive state of the eyes. Refractions are measured in the units of diopters (D). Myopia is

recognized by negative refractions and hyperopia is recognized by positive refractions. The photorefractor uses an infrared light source and a camera. The infrared light sources are arranged eccentric to the lens of the camera. When the light enters an emmetropic (normal) eye, it is reflected off the fundus and is refocused back to the light source. However, in a myopic eye the light is focused in front of the retina which will make the light reflected from the fundus spread out into a cone in which the angle depends on the amount of the relative defocus (Schaeffel, Farkas et al. 1987). In a myopic eye, the reflected light will appear brighter at the bottom of the pupil and in a hyperopic eye, the reflected light will be brighter at the top of the pupil. In case of the mouse eye, refractive measurements appear hyperopic. It is theorized that the light is reflects off the inner limiting membrane of the retina rather than the outer limiting membrane, artificially making the eye appear smaller or hyperopic. . This makes. This theory is called the small eye artifact (Glickstein and Millodot 1970)

Visual function

During progression of myopia, the functional ability of the retina may change. Hence it is of interest to measure visual function of the eye after myopia induction. The most commonly measured aspects of visual function are visual acuity and contrast sensitivity. Visual acuity refers to the spatial limit of visual discrimination. It measures functional integrity of the eye. Visual acuity measurements involve determinations of the thresholds of separation between two points. Visual acuity can represent several indications such as photochemical transduction in the retinal receptors, sorting and transmission of neural signals in the retina and visual pathways, and higher cortical processing (Westheimer 2003). It is measured using sinusoidal grating called spatial frequency and its units are measured in cycles/degree.

Contrast sensitivity is a measure of the contrast of the image. It offers a number of subtle levels of vision, not accounted for by the visual acuity test. Hence it allows a more accurate quantification of the loss of vision in a number of diseases such as cataracts, corneal edema, and neuroophthalmic diseases (Miller 2003). Contrast is the difference in the luminance of a target against background.

$$\text{Contrast} = \frac{(\text{Target luminance} - \text{Background luminance})}{(\text{Target luminance} + \text{Background luminance})}$$

Contrast threshold is presented in arbitrary units.

Optokinetic testing is a non-invasive technique, widely used for the evaluation of visual function in rodents. When an image is displaced on the retina, it results in blurring of vision if there were no gaze stabilization mechanisms. Optokinetic reflex is one of the mechanisms that helps image stabilization. Optokinetic response (OKR) is sensitive to slow motions and can react to constant velocity. OKR occurs due to the asymmetry between opposite directions during monocular stimulation. In most species temporo-nasal motion and upward motion elicit higher responses to the stimulus than the opposite directions. Lateral eyed animals (eyes on each side of head) possess strong asymmetries because asymmetries facilitate a suppression of optokinetic drive during forward locomotion because forward locomotion leads to naso-temporal optic flow on the retina. Insensitivity for naso-temporal optic flow could make the optokinetic response more sensitive for rotational movements and help to maximize gaze stabilization during head turns (Masseck and Hoffmann 2009).

Optokinetic tracking stimulation is produced by rotating stimuli around the animal. In our experiments, mice are placed on a relatively small, high platform. The stimuli are presented on four computer monitors arranged in a rectangle around the platform (Figure 3A). The stimuli are rotated horizontally in either clockwise or anticlockwise direction (Figure 3B). This stimulus

invokes a slow head turn along the direction of the stimulus. Another possible response is slow eye movements with quick repositioning fast phases in the opposite direction, also called saccades. The eye movements are called optokinetic nystagmus (OKN) and the head movements are called optokinetic tracking. Both these behaviors are reflexes and do not require training. Similar sub-cortical neural pathways are used by both behaviors (Douglas, Alam et al. 2005). Measuring OKN can be difficult as the head must be constrained so that the eyes can be viewed and eye movements recorded and analyzed using sophisticated software. Measuring optokinetic tracking is easier in that the animals are not restrained and the gross head tracking is easily observed.

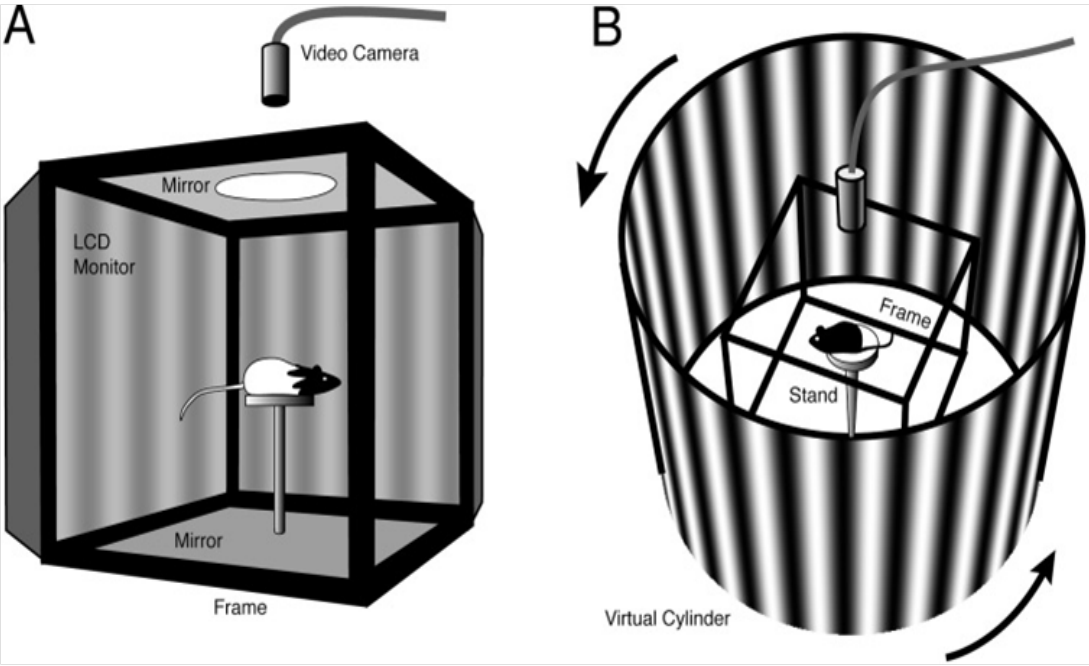

Figure 3. Optokinetic tracking system for measuring visual acuity and contrast sensitivity. (A) Virtualsystem to measure optokinetic tracking with a rat on the pedestal, (B) The appearance of stimulus on the monitor screens to the mouse. Reprinted from Visual Neuroscience, 22, Douglas, R. M., N. M. Alam, et al., Independent visual threshold measurements in the two eyes of freely moving rats and mice using a virtual-reality optokinetic system, 680, Copyright (2005), with permission from Cambridge University Press.

Previously, a non-invasive measurement of visual threshold in rats and mice was accomplished using a method called visual water task (VWT). This method uses water to provide a non-adaptive motivation and also enables the independent testing of the two eyes using cone-shaped occluders. However, it has some major drawbacks. VWT requires two weeks to train an animal and then determine one threshold. It cannot be used to study fast changing phenomena such as those occurring early in development. Also, it is impractical to measure large number of animals quickly. VWT consistently measures higher visual thresholds than the OKT and it is proposed that this is due to the retina using two different pathways. VWT is more sensitive in using the geniculo-cortical pathways while the OKT uses sub-cortical pathways. However, the results from both of these methods are found to be highly correlated (Douglas, Alam et al. 2005).

Like the VWT, OKT also provides the opportunity to test each eye independently. Binocular vision is established when ipsilateral projections from each eye reach the cortex. Although there are small ipsilateral projections in mice it does not seem sufficient to confer binocularity to the mouse optokinetic system (Douglas, Alam et al. 2005).

Objectives:

Although formation of myopia is evident with refractive measurements, it is unknown how mice perceive images after myopia development. When compared to other animals, diffusers induce relatively smaller refractions in mice. This is attributed to the low optical quality and low visual acuity of the mouse eye. The natural optical quality is so poor in a mouse eye that diffusers can degrade the retinal image only a little further (Schmucker and Schaeffel 2006). Due to this concern, it would be interesting to examine and compare the changes of visual information perceived by mice eyes to relative refractions.

The aims of this study are two-fold:

(1) Compare visual function of WT and *nob* to examine differences attributed to the ON pathway.

(2) Quantify the amount of change of visual function to relative refractions in two different strains of mice after myopia induction: WT and *nob* mice on a C57BL/6J background.

Hypothesis:

(1) The visual function of *nob* will be less than WT throughout the experiment due to the absence of the ON pathway.

(2) The visual function of the goggled eyes of both strains will degrade after myopia formation.

Materials and methods:

Animals:

This study included 6 C57BL/6J WT mice and 9 *nob* mice. The age range of WT mice was 27-56 days while the age range of *nob* mice was 27-42 days . Animals were bred at the Atlanta VA Medical center. Mice were housed with their mothers until weaning which is postnatal day 21. The animal facility undergoes a 12-hour light/dark cycle. The control right eye is OD, and control left eye is OS. The ungoggled eye is called opposite.

Experimental design:

Mice were first measured for baseline visual acuity, contrast sensitivity and refractions under anesthesia (asleep refractions) at P27. Animals from both strains were split into two groups: control and goggled. The goggled group underwent surgery and goggling of the right

eye. Animals were checked every day to see if goggles were covering the eyes. Previous studies (Pardue, Faulkner et al. 2008) have shown that *nob* mice develop form deprivation myopia in 2 weeks whereas WT mice takes 4-6 weeks. After 2 and 4 weeks, myopia was confirmed in *nob* and WT mice, respectively, with refractive errors, visual acuity and contrast sensitivity measured.

OKT:

Optokinetic tracking was measured using a virtual optomoter system called OptoMotry(Prusky, Alam et al. 2004). Mice were placed on a platform in the center of four computer monitor screens arranged in a rectangle (Figure 3). The visual stimuli were presented on the screens in either clockwise or anti-clockwise direction. A camera was placed above the mouse to view the head turns in response to the moving grating. A computer program was used to vary the spatial frequency or contrast sensitivity of sinusoidal waves on the monitor screens. The luminance inside the machine was set to 30 cd/cm^2. Measurements were taken at the beginning of dark cycle of the animal. Visual acuity was measured starting from 0.042 cyc/deg until a threshold was reached. The contrast sensitivity was measured at 5 spatial frequencies 0.031, 0.064, 0.103, 0.192 and 0.272 cyc/deg. The values of contrast were measured in percentage using the formula mentioned above. For data analysis, these values were converted by a Michealson conversion factor using the equation:

y= 35.647*x^(-0.80632).

This enabled accurate measurements as the monitor screens used in the OptoMotry system cannot emit 100% black and white. A cursor was placed in between the eyes of the animal to adjust the viewing distance of the stimuli such that the animal was in the center of the virtual

drum created by the monitors. The experimenter viewed the animal from the top and made one of two choices: Yes, for tracking in the direction of the moving stimulus and No, for any other random movements. Contrast sensitivity data was analyzed using a three-factor ANOVA to determine if there were significant changes among spatial frequencies, time and treatment. After confirming a significant three-way interaction, a two-factor ANOVA was performed to measure significance between spatial frequencies and treatment at the final timepoint only. Visual acuity data was analyzed using a two-factor ANOVA to measure significance between treatment (goggled, opposite, control) and time (baseline and final timepoint). Post-hoc comparisons were performed with Holm-Sidak analysis.

Photorefraction:

An eccentric photorefractor modified for the mouse eye was used to measure refractive errors in mice (Schaeffel, Farkas et al. 1987). Prior to refraction the animals were weighed and tropicamide was applied to their eyes to ensure pupil sizes greater than 2 mm. To measure asleep refractions, mice were anaesthetized with ketamine/xylazine (80 mg/kg; 16 mg/kg). Mice were placed on a platform and positioned in front of the camera lens at a distance of approximately 60cm. When the purkinje image of the cornea is within 3 degrees of the central optical axis of the eye and centered within the pupil, the computer software takes 10 images of the eye within 1 msec. After measuring the asleep refractions, 0.05 ml of yohimbine (2.1 mg/kg) was given to mice for recovery. The software automatically uploads the values in an excel spreadsheet for further analysis. Two factor ANOVA was performed to measure significance of the treatment groups (goggled, opposite, control) across time (baseline and final timepoint). Post-hoc comparisons were performed with Holm-Sidak analysis.

Surgery:

Surgery was performed on animals at P27. Mice were sedated with ketamine/xylazine (80 mg/kg; 16mg/kg) and their heads were shaved between their ears. Surgery was performed on a heating pad and eyes were kept moist by applying saline drops (0.9% NaCl). Using a scalpel blade, a small vertical incision was made at the center to view the sagittal and lambda sutures of the skull. The skin around the sutures was removed with surgical scissors. The exposed fascia and periosteum were removed. Using a bone drill, with a 0.7 mm blur, three holes were drilled, one on each region created by the sutures. Using a screwdriver, 4 mm stainless screws were carefully inserted into the drilled holes. Cyanoacrylate glue was applied over the screws and was allowed to dry. A semi-solid mixture of dental cement was applied over the dried glue and molded to completely cover the skull. Before curing, a metal tube was placed over the dental cement parallel to the dorsal axis of the mouse. Finally, a small quantity of dental cement was added over the tube and was allowed to dry. Immediately following surgery, mice were injected with .10 ml of NaCl and 0.05 ml of metacam to recover. The remaining components of the apparatus such as the goggle and balancing bar were inserted into the acrylic cube and tightened with a screw (Figure 4) (Faulkner, Kim et al. 2007).

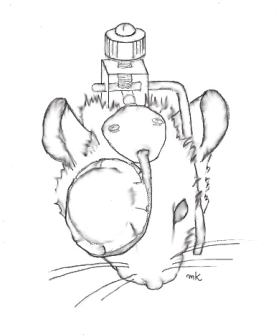

Figure 4. Appearance of a mouse after goggle placement. The sketch shows the placement of the goggle, acrylic cube and balancing bar. Reprinted from Journal of Neuroscience Methods, 161, Faulkner, A., M. Kim, et al., Head-mounted goggles for murine form deprivation myopia, 97, Copyright (2007), with permission from Elsevier.

Results:

Refractive development:

Ungoggled WT eyes of control OD had hyperopic refractions from baseline to 4 weeks of age, ranging from 4.25 ± 0.57 to 5.79 ± 0.64. Goggling produced a significant difference between the two treatment groups by 4 weeks (Figure 5; two-factor, repeated measures ANOVA $F(3, 23) = 7.491$, $p<0.010$). The diffuser goggle induced a significant myopia shift at 4 weeks compared to the opposite eyes of the same animals and naïve, control animals (post hoc comparisons, $p<0.0001$)

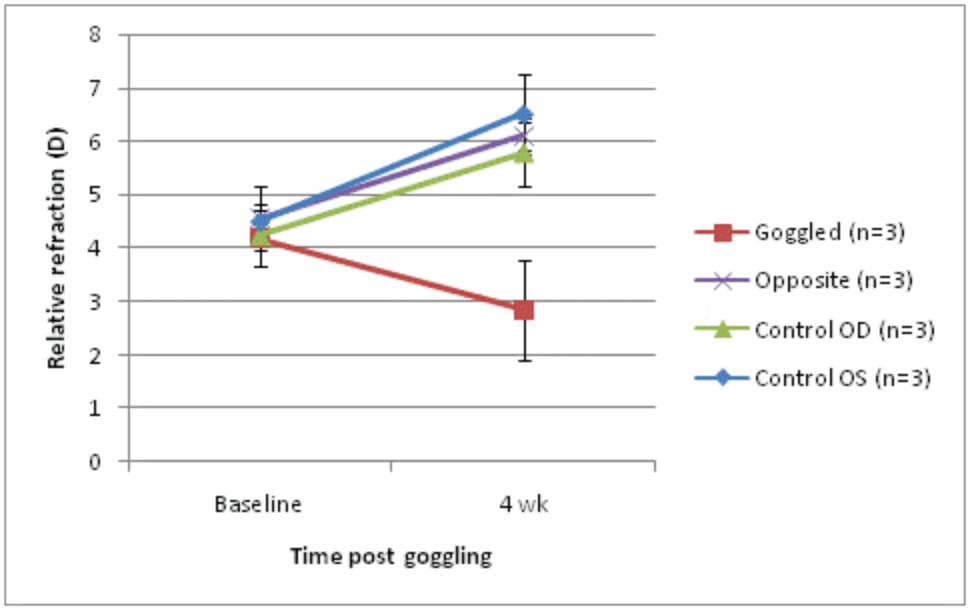

Figure 5. Refractive development of WT mice from baseline to 4 weeks measured with a photorefractor. The goggled eyes of WT mice developed a significant myopic shift after 4 weeks. Data are expressed as the mean ± standard deviation.

Nob mice under normal conditions also had hyperopic refractions at the ages examined. For example, the control OD shifted from 5.23 ± 0.23D at baseline to 7.40 ± 0.71 (Figure 6). As previously reported, *nob* mice developed a significant myopic shift by 2 weeks after form deprivation goggling (Figure 6; two-factor, repeated measures ANOVA $F(3, 35) = 22.826$, $p<0.001$). The refractive error of goggled eyes at 2 weeks was 2.69±0.69 and was significantly different from opposite eyes (7.33 ± 0.55 cyc/deg), control OD (7.39 ± 0.71 cyc/deg; post hoc comparison, $p<0.0001$), and control OS (7.91 ± 1.12cyc/deg) eyes.

A comparison of WT and *nob* mice showed that the goggled eyes of *nob* mice developed myopia by 2 weeks compared to WT mice which took 4 weeks. Also note that the difference in myopic shift was greater in *nob* mice compared to WT, even with the shorter goggling period. The difference in refractive error change of WT at 4 weeks was 3.28 ± 0.79D. The difference in refractive error change of *nob* at 2 weeks was 4.86 ± 0.71D.

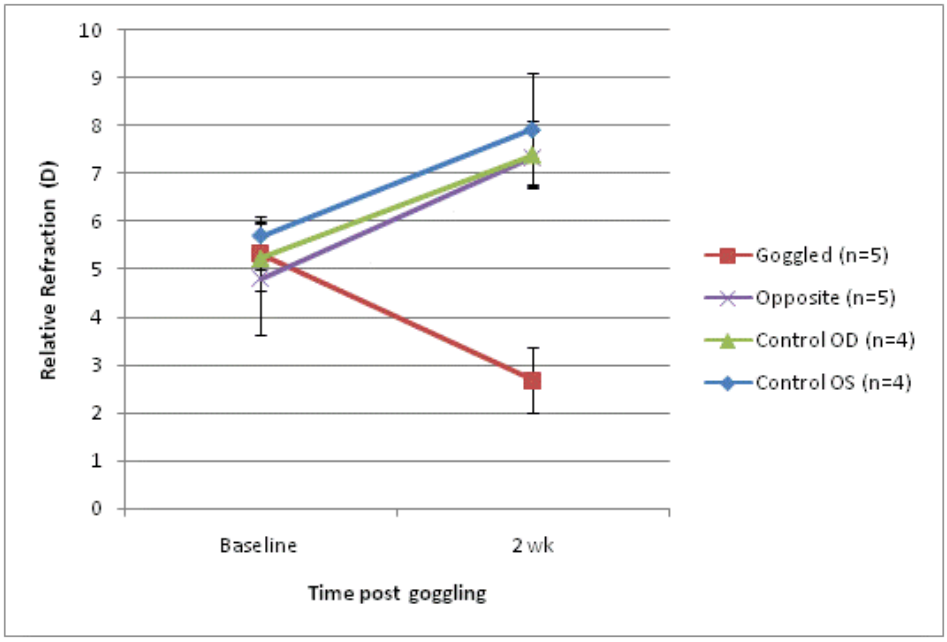

Figure 6. Refractive development of *nob* mice from baseline to 2 weeks measured with a photorefractor. The goggled eyes of *nob* mice developed a significant myopic shift after 2 weeks. Data are expressed as the mean ± standard deviation.

Visual Acuity

Visual acuity of control WT mice remained constant through the experiment. The visual acuity of control and goggled eyes did not significantly differ from baseline to 4 weeks after form deprivation (Figure 7). The spatial frequencies of goggled eyes were similar to opposite, OD and OS eyes after 4 weeks when a myopic shift was detected.

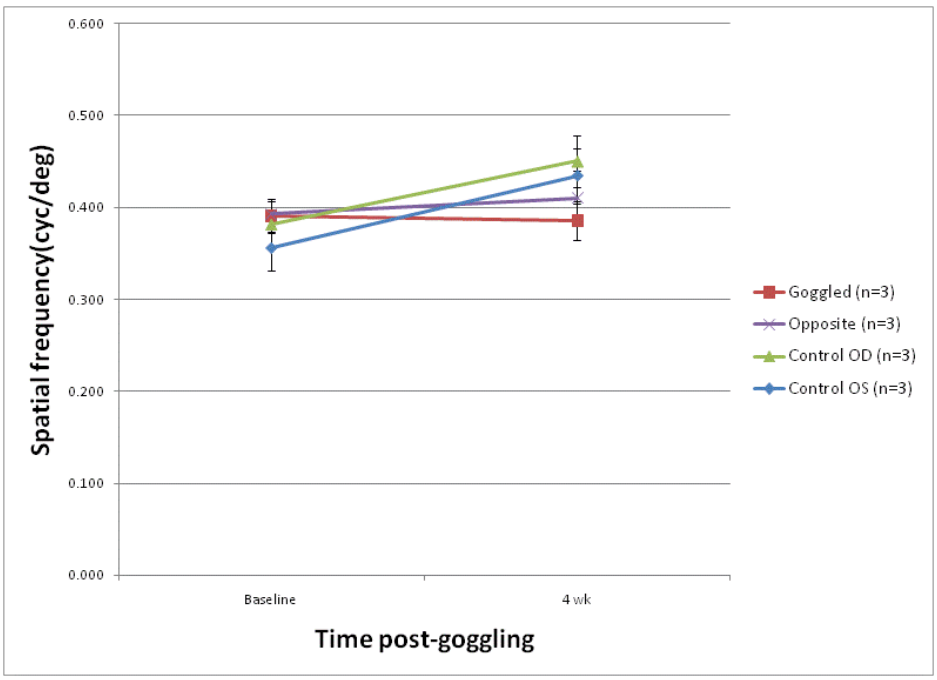

Figure 7. The visual acuity of WT mice from baseline to 4 weeks measured with OKT. The visual acuity of goggled eyes from WT mice did not significantly change compared to the opposite and control eyes. Data are expressed as the mean ± standard deviation.

The visual acuity of control OD *nob* mouse eyes increased from 0.32 ± 0.02cyc/deg to 0.45 ± 0.03cyc/deg from P28 to P42. The visual acuity of goggled *nob* mouse eyes was significantly lower than opposite eyes and eyes from control mice after 2 weeks (Figure 8; two-factor, repeated measured ANOVA $F(3, 35) = 8.210$, $p<0.002$; post-hoc comparison, $p<0.0001$). The spatial frequencies of all ungoggled eyes increased overtime; however, the spatial frequency threshold of goggled eyes after myopic shift remained constant. The visual acuity threshold of the goggled eye was 0.32 ± 0.02cyc/deg at baseline and 0.34 ± 0.03 at 2 weeks.

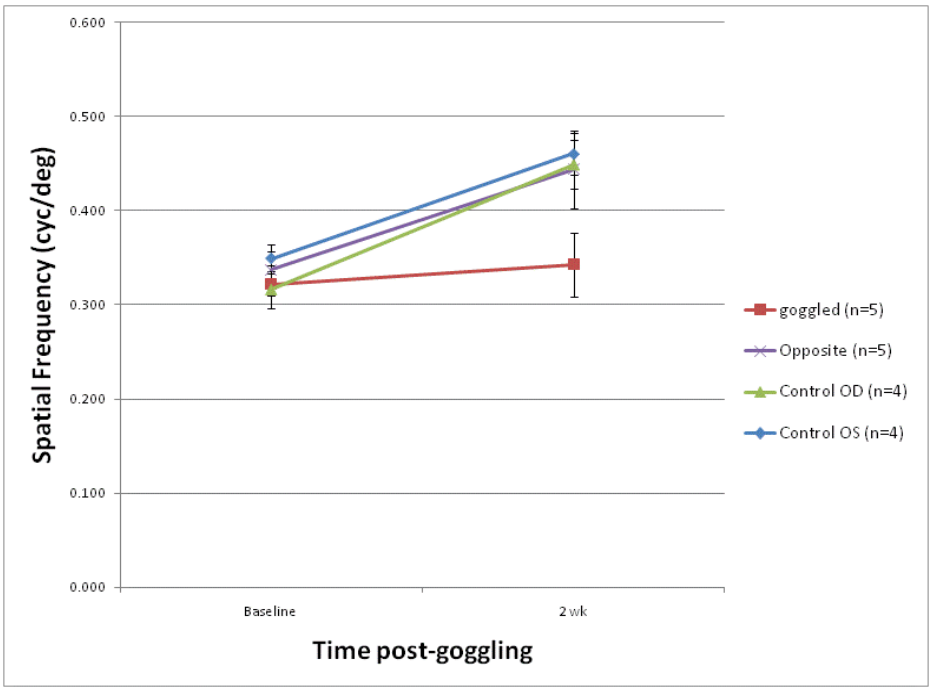

Figure 8. The visual acuity of *nob* mice from baseline to 2 weeks post-goggling measured with OKT. The visual acuity of goggled eyes from *nob* mice was significantly shifted when compared to control eyes and opposite eyes. Data are expressed as the mean ± standard deviation.

Contrast Sensitivity:

The contrast sensitivity curve of WT control mice (OD) after 4 weeks remained similar to the baseline values at all spatial frequencies (Figure 9). The contrast sensitivity of goggled eyes in WT mice at 4 weeks is not significantly different from OD. The opposite eye and control OS were similar to baseline (Figure not shown). Control OD and goggled eyes did not change and were found to be similar to control OS and opposite.

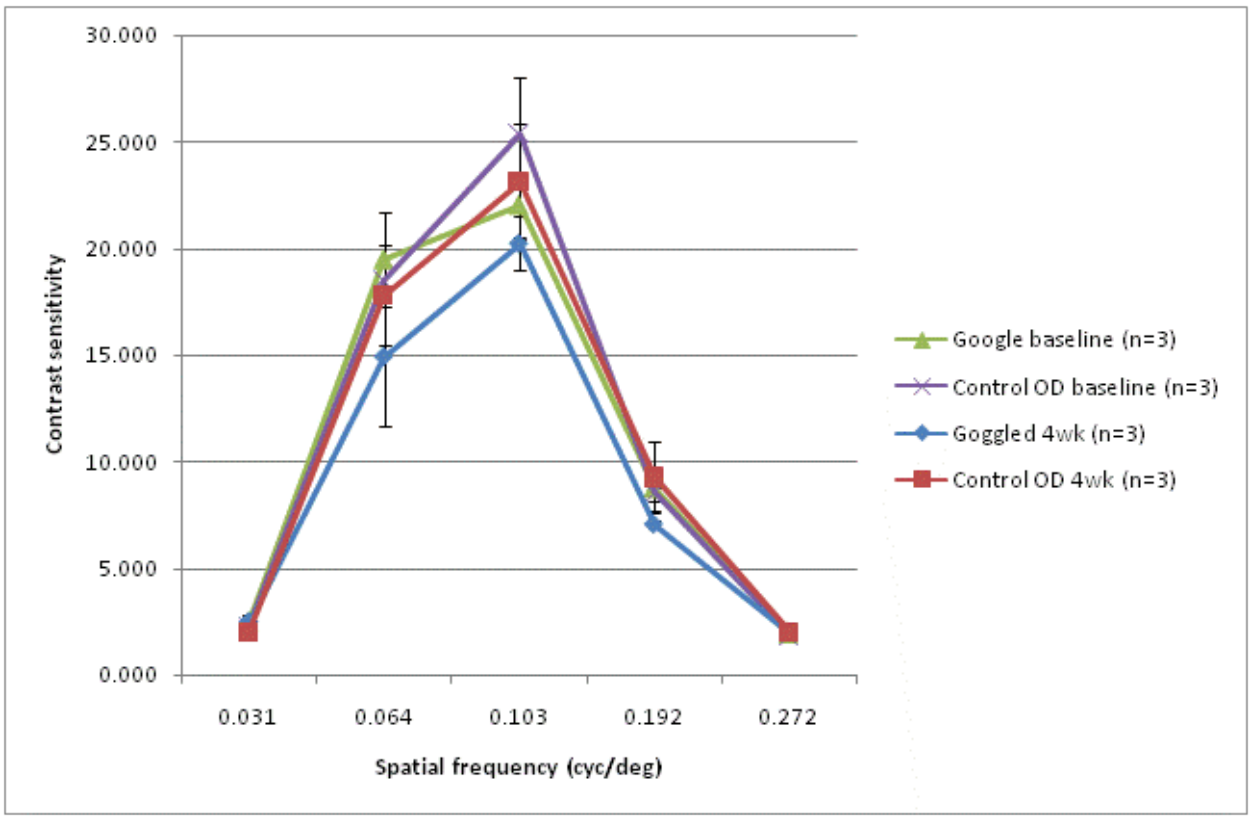

Figure 9. The contrast sensitivity of WT mice as indicated at baseline and at 4 weeks as measured with OKT. The contrast sensitivity of the goggled eyes was not significantly different from the control group. Data are expressed as the mean ± standard deviation.

The control *nob* mice increased in contrast sensitivity after 2 weeks. From Figure 10, contrast sensitivity of control OD *nob* eyes increases from 8 to 11 units at 0.103cyc/deg and 4 to 9 units at 0.064cyc/deg when comparing baseline to 2 week values. The contrast sensitivity of goggled *nob* mice was significantly lower after 2 weeks compared to baseline and the control *nob* mice (three-factor, repeated measurements ANOVA $F(12, 56) = 9.930$, $p<0.001$). After myopic shift, the goggled eyes significantly decreased in contrast sensitivity at 0.103cyc/deg (post hoc comparison, $p<0.0001$).

The contrast sensitivity of opposite and control OS *nob* eyes showed the same trends as the control OD and were not significantly different from each other (data not shown).

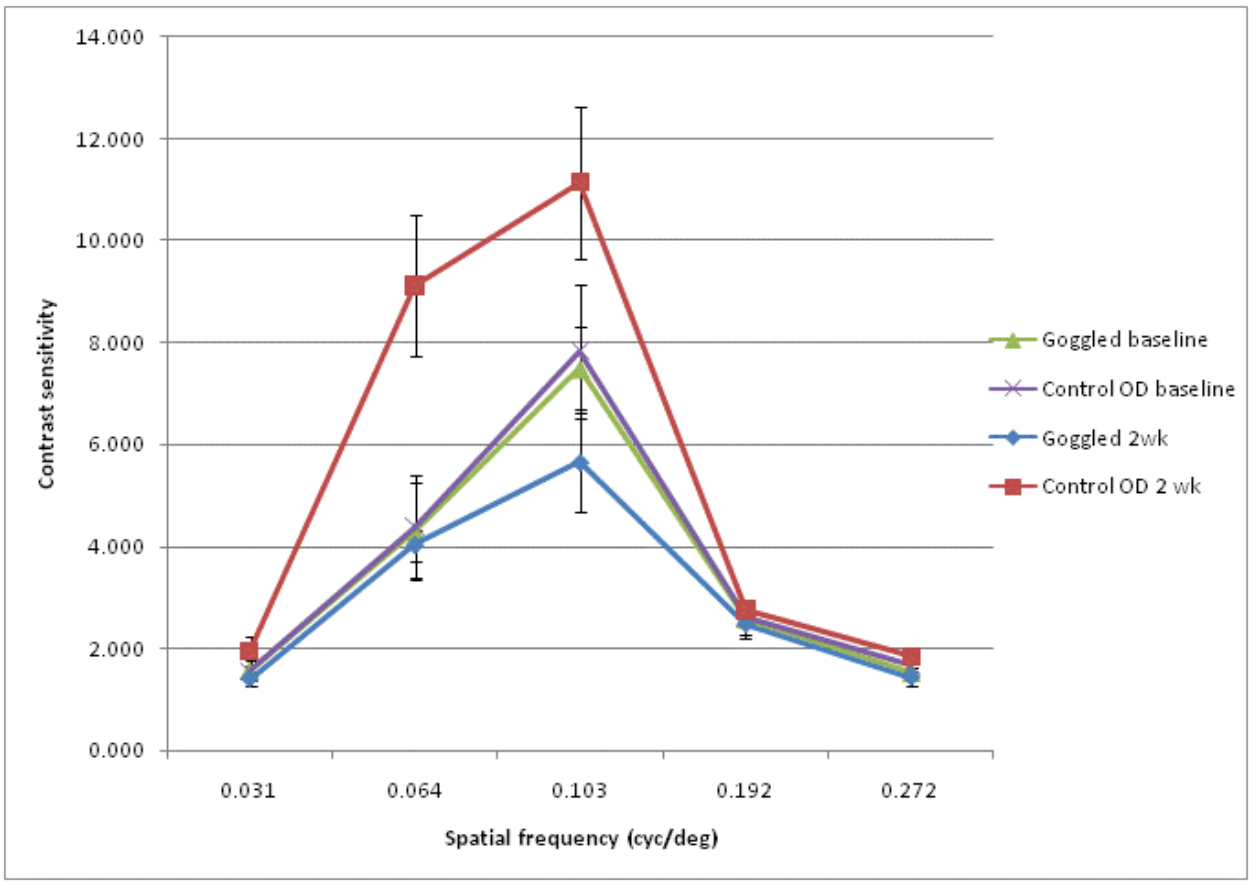

Figure 10. The contrast sensitivity of *nob* mice at baseline and at 2 weeks measured with OKT. The contrast sensitivity of the goggled eye significantly shifted from OD of control group. Data are expressed as the mean ± standard deviation.

Nob vs. WT

The goggled eyes of *nob* mice developed less hyperopic refractions (myopic shift) of 5.32 ± 0.78D at 2 weeks from a baseline of 2.68 ± 0.69D (Figure 6). The goggled eyes of control WT mice developed less hyperopia (2.85 ± 0.93D) at 4 weeks compared to baseline values (4.18 ± 0.51D; Figure 5).

Visual acuity of *nob* mice at baseline was lower when compared to WT. At baseline, the average visual acuity of *nob* mice is 0.33 ± 0.02cyc/deg compared to 0.38 ± 0.02cyc/deg in WT mice (Figures 7 and 8).

The highest contrast sensitivity was measured at a spatial frequency of 0.103cyc/deg at baseline and after myopic shift, in both strains of mice. The most sensitive spatial frequencies for contrast were 0.064 and 0.103cyc/deg (Figure 9 and 10).

The *nob* mice had a lower contrast sensitivity overall when compared to WT. The highest contrast sensitivity of *nob* was 10 units at spatial frequency 0.103cyc/deg (Figure 10). The highest contrast sensitivity of WT is 25 units at a spatial frequency of 0.103cyc/deg (Figure 9).

Discussion:

Refractions:

In this experiment, goggled eyes of WT mice (Figure 5) and *nob* mice (Figure 6) achieved significant myopic refractions after undergoing form deprivation for 4 weeks and 2 weeks, respectively. However, goggled eyes of *nob* mice attained a higher myopic shift compared to that of WT in a shorter period of time. This is likely due to the ON pathway defect in the retina of *nob* mice. This result is supported by a previous study (Pardue, Faulkner et al. 2008) where *nob* mice reached a significant myopic shift sooner than WT. In this previous study, the WT mice were followed for a longer period of time, till 6 weeks, and the amount of myopic shift in *nob* and WT was approximately equal (~ 4 D). In this study, due to time constraints, measurements were taken at 4 weeks after goggling in WT mice and a 3.28 ± 0.79D myopic shift was noticed compared to 4.86 ± 0.71D in *nob* mice.

Visual Acuity:

Visual acuity of WT mice seems to be generally higher than that of *nob* mice (Figure 7 & Figure 8). While *nob* mice have a defect in the ON pathway, their visual acuity was surprisingly good compared to WT values. The baseline visual acuity of *nob* mice was 0.33 ± 0.02 cyc/deg, while the baseline visual acuity of WT was 0.038 ± 0.02cyc/deg. This is consistent with CSNB1

patients who retain reasonably good visual acuity, light sensitivity and color vision under daylight conditions (Miyake, Yagasaki et al. 1986). The difference in visual acuity is due to the ON pathway defect which compromises the signaling in the rod pathway and partially in the cone pathway (Pardue, McCall et al. 1998). Since the measurements are taken under photopic conditions, the suspected pathway responsible for this difference is probably the cone-ON bipolar pathway (see Figure 2). However, one study conducted experiments with cone knockout mice and rod knockout mice and noticed that the visual acuity of cone-only models in photopic conditions was 0.2 cyc/deg compared to WT, which was 0.3cyc/deg. They suggested that the peak visual performance in photopic conditions is obtained when rod pathway is functional (Schmucker, Seeliger et al. 2005). Further experiments should be conducted to find out the specific contributions of rod and cone pathway to visual acuity.

In WT mice the visual acuity remained unchanged after form deprivation (Figure 7). The WT mice started with a high visual threshold at baseline and no difference in visual acuity was apparent after a 3.2 D myopic shift. This myopic shift may not be sufficient to detect a decrease in visual acuity in WT mice. As seen in Figure 3, a slow decrease in visual acuity was noticed in WT mice (Figure 7) but did not reach significance, suggesting that a longer period of goggling may have produced a greater myopic shift and a significant decrease in visual acuity.

After myopia development, the visual acuity of goggled *nob* eyes remained constant whereas opposite and control eyes increased (Figure 8). Hence, the difference between goggled and control/opposite eyes showed a decrease in visual acuity at the end of form deprivation. This study hypothesized that the visual acuity of *nob* mice would degrade after form deprivation. However, the results indicate that the myopic shift of 4.8 D caused a decrease in visual acuity

overtime, relative to the opposite and control eyes, but did not degrade visual acuity from the initial value.

While comparing the effects of form-deprivation on the progression of visual acuity of the two strains, it was difficult to directly compare the effects since the amount of myopic shift was different. There is a possibility that some effects are obscured due to the lower myopic shift detected in WT animals. In future experiments, an equal change in myopic refractions between two strains is necessary to make appropriate comparisons.

Contrast sensitivity:

The baseline contrast sensitivity of WT animals as shown in Figure 9 had the highest sensitivity at 0.103cyc/deg. There are differing reports in the literature as to which spatial frequency produces the most sensitivity. The results from this study are in accordance with the observations in some behavioral studies which also show a high contrast close to 0.103cyc/deg (Schmucker, Seeliger et al. 2005) (Umino, Solessio et al. 2008) (Sinex, Burdette et al. 1979). Other studies suggest that highest contrast sensitivity is detected at 0.06cyc/deg using optokinetic tracking (Prusky, Alam et al. 2004) and VEP's (Porciatti, Pizzorusso et al. 1999).

The baseline contrast sensitivity of *nob* mice showed a similar peak of sensitivity at 0.103cyc/deg (Figure 10). However, the highest contrast detected by *nob* mice at this frequency is 8 units compared to 25 units in WT mice. This difference could be attributed to the absence of ON pathway in *nob* mice. As mentioned above, in *nob* mice the rod pathway, as well as a part of the cone pathway, are compromised. These pathways play a critical role in detecting contrast. Under photopic conditions, as tested here, contrast sensitivity is primarily detected by the cone

pathway (Umino, Solessio et al. 2008). Hence, it is the cone-ON bipolar pathway that is responsible for the significant decrease in contrast sensitivity at P28.

Between P28 and P56, the contrast sensitivity of WT control mice remained constant (Figure 9). In a study that measured contrast sensitivity at various ages in WT mice, maximum contrast sensitivity was reached by P28 for spatial frequencies 0.103, 0.064, 0.0192, and 0.272 (Prusky, Alam et al. 2004). In agreement with this study, the contrast sensitivity in control WT eyes remained constant between P28 and P56. After form deprivation, the goggled WT eyes did not significantly change from baseline. This could be due to a small myopic shift (3.2 D) since a trend towards decreased contrast sensitivity can be noticed in Figure 9, but it does not reach significance.

In control *nob* mice, the contrast sensitivity increased at 0.064 and 0.103cyc/deg from P28 to P42 (Figure 10). This suggests that, contrast sensitivity does not reach a threshold at P28, as found in WT mice. The developing visual system is shaped by visual experience. The ON-pathway could play a critical role in developing contrast sensitivity at early ages in WT animals. Moreover, it is unclear as to the time required by *nob* mice to reach maximum contrast threshold. Future studies should test contrast threshold at various ages in *nob* mice.

After form deprivation, the contrast sensitivity of WT mice did not significantly change and remained constant (Figure 9). As predicted in this study, the contrast sensitivity curve of *nob* mice significantly decreased after a myopic shift (Figure 10). This data suggests that *nob* mice are more susceptible to contrast degradation probably due to the ON pathway defect. Another possibility is that the continued increase in contrast sensitivity of control *nob* eyes with age produced a greater difference in sensitivity thresholds between the goggled and control/opposite *nob* eyes.

In conclusion, the first hypothesis that visual function of *nob* will be less than WT throughout the experiment is supported by the results. The second hypothesis that the visual function of the goggled eyes of both strains will degrade after myopia formation was not entirely supported. The visual function and contrast sensitivity of WT did not degrade after form deprivation; they remained constant. The visual function of *nob* mice showed a decrease after form deprivation, relative to the opposite/control eyes, but did not decrease from baseline which may indicate a degenerative process. These results support the important role of the ON pathway in refractive development, contrast sensitivity, and visual acuity.

References:

Boatright, J. H., J. R. Gordon, et al. (1994). "Inhibition of endogenous dopamine release in amphibian retina by L-2-amino-4-phosphonobutyric acid (L-AP4) and trans-2-aminocyclopentane-1,3-dicarboxylate (ACPD)." Brain Res **649**(1-2): 339-342.

Cohen, S. Y., A. Laroche, et al. (1996). "Etiology of choroidal neovascularization in young patients." Ophthalmology **103**(8): 1241-1244.

Douglas, R., N. Alam, et al. (2005). "Independent visual threshold measurements in the two eyes of freely moving rats and mice using a virtual-reality optoinetic system." Visual Neuroscience **22**: 677-684.

Economics, A. (2004). Clear Insight - The Economic Impact and Cost of Vision Loss in Australia, Eye Research Australia.

Faulkner, A., M. Kim, et al. (2006). "Head-mounted goggles for murine form deprivation myopia." J Neurosci Methods **161**: 96-100.

Feldkaemper, M., S. Diether, et al. (1999). "Interactions of spatial and luminance information in the retina of chickens during myopia development." Exp Eye Res **68**(1): 105-115.

Gentle, A., Y. Liu, et al. (2003). "Collagen gene expression and the altered accumulation of scleral collagen during the development of high myopia." J Biol Chem **278**(19): 16587-16594.

Glickstein, M. and M. Millodot (1970). "Retinoscopy and eye size." Science **168**(931): 605-606.

Gregg, R. G., S. Mukhopadhyay, et al. (2003). "Identification of the gene and the mutation responsible for the mouse nob phenotype." Invest Ophthalmol Vis Sci **44**(1): 378-384.

Hayashi, H., K. Yamashiro, et al. (2011). "Association of 15q14 and 15q25 with High Myopia in Japanese." Invest Ophthalmol Vis Sci.

Hess, R., K. Schmid, et al. (2006). "What image properties regulate eye growth?" Curr. Biol. **16**: 687-691.

Khor, C. C., Q. A. Fan, et al. (2010). "Support for TGFB1 as a Susceptibility Gene for High Myopia in Individuals of Chinese Descent." Archives of Ophthalmology **128**(8): 1081-1084.

Liang, C. L., E. Hsi, et al. (2011). "A functional polymorphism at 3' UTR of the PAX6 gene may confer risk for extreme myopia in Chinese." Invest Ophthalmol Vis Sci.

Marsh-Tootle, W. L. and T. T. Norton (1989). "Refractive and structural measures of lid-suture myopia in tree shrew." Invest Ophthalmol Vis Sci **30**(10): 2245-2257.

Masseck, O. A. and K. P. Hoffmann (2009). "Comparative Neurobiology of the Optokinetic Reflex." Basic and Clinical Aspects of Vertigo and Dizziness **1164**: 430-439.

Miller, D. (2003). Physiologic Optics and Refraction. Physiology of the Eye. P. L. Kauman, Alm, Albert.,. St. Louis, Mosby. **10**.

Miyake, Y., K. Yagasaki, et al. (1986). "Congenital stationary night blindness with negative electroretinogram. A new classification." Arch Ophthalmol **104**(7): 1013-1020.

Morgans, C. W., G. Ren, et al. (2006). "Localization of nyctalopin in the mammalian retina." Eur J Neurosci **23**(5): 1163-1171.

Pardue, M. T., A. E. Faulkner, et al. (2008). "High susceptibility to experimental myopia in a mouse model with a retinal on pathway defect." Invest Ophthalmol Vis Sci **49**(2): 706-712.

Pardue, M. T., M. A. McCall, et al. (1998). "A naturally occurring mouse model of x-linked congenital stationary night blindness." Investigative Ophthalmology & Visual Science **39**(12): 2443-2449.

Porciatti, V., T. Pizzorusso, et al. (1999). "The visual physiology of the wild type mouse determined with pattern VEPs." Vision Research **39**(18): 3071-3081.

Prusky, G. T., N. M. Alam, et al. (2004). "Rapid quantification of adult and developing mouse spatial vision using a virtual optomotor system." Investigative Ophthalmology & Visual Science **45**(12): 4611-4616.

Qian, Y. S., R. Y. Chu, et al. (2009). "Incidence of Myopia in High School Students with and without Red-Green Color Vision Deficiency." Investigative Ophthalmology & Visual Science **50**(4): 1598-1605.

Rada, J. A. S., S. Shelton, et al. (2006). "The sclera and myopia." Experimental Eye Research **82**(2): 185-200.

Saw, S. M., G. Gazzard, et al. (2005). "Myopia and associated pathological complications." Ophthalmic Physiol Opt **25**(5): 381-391.

Schaeffel, F. (2006). "Myopia: the importance of seeing fine detail." Current Biology **16**(7): R257-259.

Schaeffel, F. and S. Diether (1999). "The growing eye: an autofocus system that works on very poor images." Vision Res **39**(9): 1585-1589.

Schaeffel, F., L. Farkas, et al. (1987). "Infrared Photoretinoscope." Applied Optics **26**(8): 1505-1509.

Schaeffel, F., D. Troilo, et al. (1990). "Developing Eyes That Lack Accommodation Grow to Compensate for Imposed Defocus." Visual Neuroscience **4**(2): 177-183.

Schmucker, C. and F. Schaeffel (2006). "Contrast sensitivity of wildtype mice wearing diffusers or spectacle lenses, and the effect of atropine." Vision Res **46**(5): 678-687.

Schmucker, C., M. Seeliger, et al. (2005). "Grating acuity at different luminances in wild-type mice and in mice lacking rod or cone function." Investigative Ophthalmology & Visual Science **46**(1): 398-407.

Sinex, D. G., L. J. Burdette, et al. (1979). "Psychophysical Investigation of Spatial Vision in the Normal and Reeler Mutant Mouse." Vision Research **19**(8): 853-857.

Stone, R. A., T. Lin, et al. (1989). "Retinal dopamine and form-deprivation myopia." Proc Natl Acad Sci U S A **86**(2): 704-706.

Troilo, D., M. D. Gottlieb, et al. (1987). "Visual deprivation causes myopia in chicks with optic nerve section." Curr Eye Res **6**(8): 993-999.

Umino, Y., E. Solessio, et al. (2008). "Speed, spatial, and temporal tuning of rod and cone vision in mouse." Journal of Neuroscience **28**(1): 189-198.

Wallman, J. and J. Winawer (2004). "Homeostasis of eye growth and the question of myopia." Neuron **43**(4): 447-468.

Westheimer, G. (2003). Visual Acuity. Physiology o the Eye. P. L. Kaufman, Alm, A.,. St. Louis, Mosby. **10**.

Wu, S. Y., B. Nemesure, et al. (1999). "Refractive errors in a black adult population: The Barbados Eye Study." Investigative Ophthalmology & Visual Science **40**(10): 2179-2184.